

A new memristor-based low-pass filter topology and its small-signal solution using MacLaurin series

SUAYB CAGRI YENER^{a,*}, RESAT MUTLU^b, H. HAKAN KUNTMAN^c

^a*Sakarya University, Engineering Faculty, Electrical and Electronics Engineering Department 54187, Sakarya, Turkey*

^b*Namik Kemal University, Corlu Engineering Faculty, Electronics and Communication Engineering Department, 59860, Corlu, Tekirdag, Turkey*

^c*Istanbul Technical University, Electrical – Electronics Faculty, Electronics and Communication Engineering Department 34469, Maslak, Istanbul, Turkey*

In this work, a new memristor-based low-pass filter topology is suggested. Memristor-based filters are nonlinear circuits and many of them cannot be solved analytically. To find an approximate analytical solution of the filter equations, MacLaurin series is used for the first time. Time and frequency domain behavior of the filter are obtained. Also, the frequency domain gain and total harmonic distortion characteristics of the filter are given. Results obtained by the small signal model have been compared with the dynamic model results. It is shown that the small signal model is able to predict the filter behavior very well.

(Received March 9, 2014; accepted January 21, 2015)

Keywords: TiO₂ memristor, Low-pass filter, Memristor-based filter, Dynamical model, Small-signal analysis, Total harmonic distortion, Maclaurin series

1. Introduction

Memristor has been claimed as a fundamental circuit element by Chua in 1971 and a memristive device behaving as a memristor has been discovered in 2008 [1, 2]. The new circuit element has zero-crossing hysteresis loop under AC excitation, a charge dependent resistance (memristance) and a saturation mechanism which cannot be mimicked by other fundamental circuit elements such as resistor, capacitor and inductor [1, 3]. Because of these properties, it is a candidate for both analog and digital applications. Memristor has already been used in programmable filters, programmable gain amplifiers, integrators, controllers and oscillators [4-7]. Some applications of filters with memristors are previously presented in the literature [8-20].

In this study, a new low pass filter which has a memristor placed as the input element and a resistor-capacitor parallel circuit placed as the negative feedback to an inverting op-amp is proposed. The resistor-capacitor parallel circuit provides a constant cut-off frequency and the memristor provides adjustable gain characteristic. Memristor is a nonlinear circuit element and, therefore, memristor-based circuits are also nonlinear. Many of them cannot be solved analytically. To solve the proposed filter equation analytically, its small-signal analysis is done based on Maclaurin series and using linear drift TiO₂ memristor model [2]. To the best of our knowledge, Maclaurin series is used for analyzing memristor based filters for the first time in literature.

Time domain analyses are done using the small signal model and the frequency domain gain characteristic of the filter are presented. Simulation results of the small signal model have been compared with that of the dynamic model obtained numerically with SimulinkTM toolbox of MatlabTM. It is shown that the small signal model is able to predict the filter behavior well for small signals. In this work, the total harmonic distortion of the new memristor-based low-pass filter is also given as a figure of merit. It has been found out that the input signal magnitude should be limited for a low distortion at low frequencies.

This paper is organized as follows. In the second section, linear drift TiO₂ memristor model is given. In the third section, the new memristor-based low-pass filter topology is introduced and its dynamic model is given. In the fourth section, its small-signal model is obtained using McLaurin series. Also the filter gain and total harmonic distortion (THD) formulas are also derived in this section. In the fifth section, simulation results of the filter for both of the models are presented. Its time-domain waveforms, gain and total harmonic distortion (THD) behavior are simulated and results obtained with both of the models are presented and compared in this section. Paper is finished with conclusion.

2. Linear drift model of memristor

A memristor can be modeled as either charge or flux controlled [1]. The terminal equations of the charge-

controlled and flux-controlled memristor are given in (1) and (2) respectively

$$v(t) = M(q)i(t) \quad (1)$$

$$i(t) = W(\varphi)v(t) \quad (2)$$

where $M(q)$ is the memristor's memristance and $W(\varphi)$ is the memristor's memductance, respectively. Memristor charge as the time-integration of current and flux is the integration of its voltage with respect to time and these equal to

$$q(t) = \int_{-\infty}^t i(\tau) d\tau \quad (3)$$

$$\varphi(t) = \int_{-\infty}^t v(\tau) d\tau \quad (4)$$

In this work, the charge dependent TiO_2 memristor with linear dopant drift speed model given in [2] is used. It is linearly dependent on memristor charge and their TiO_2 memristor memristance (or resistance) with linear dopant drift system is given as

$$M(q) = \frac{d\varphi}{dq} = R_{\text{OFF}} \left(1 - \frac{\mu_V R_{\text{ON}}}{D^2} q(t) \right) \quad (5)$$

In (5) D is total thickness of the thin film, μ is mobility of oxygen vacancies in memristor, R_{ON} and R_{OFF} correspond low and high state resistances, respectively. Memristance function can also be simplified as following.

$$M(q) = \frac{d\varphi}{dq} = M_0 - K_q q(t) \quad (6)$$

where $M_0 = R_{\text{OFF}}$ is the maximum memristance, K_q is the memristance charge coefficient, $q(t)$ is the instantaneous memristance charge. By integrating (6) flux is defined as the function of charge.

$$\varphi = M_0 q - \frac{K_q}{2} q^2 \quad (7)$$

The charge of the memristor is found as

$$q = \frac{M_0 - \sqrt{M_0^2 - 2K_q \varphi}}{K_q} \quad (8)$$

Its current is:

$$i(t) = \frac{dq(t)}{dt} = \frac{\frac{d\varphi(t)}{dt}}{\sqrt{M_0^2 - 2K_q \varphi}} \quad (9)$$

For a memristor, memristor voltage is

$$v_{in} = \frac{d\varphi}{dt} \quad (10)$$

Eq. (9) turns into

$$i(t) = \frac{v(t)}{\sqrt{M_0^2 - 2K_q \varphi}} \quad (11)$$

Memristance and memductance functions of memristor are:

$$M(q) = M_0 - K_q q = \sqrt{M_0^2 - 2K_q \varphi} \quad (12)$$

and

$$W(\varphi) = \frac{1}{\sqrt{M_0^2 - 2K_q \varphi}} \quad (13)$$

Memristor flux can take values from 0 to φ_{SAT} . If the memristor is saturated at $\varphi=0$, its memristance and memconductance are equal to M_0 and $W_0=1/M_0$ respectively. If the memristor is saturated at $\varphi=\varphi_{\text{SAT}}$, its memristance and memductance are equal to

$$M_{\text{SAT}} = M_0 - K_q q_{\text{SAT}} = \sqrt{M_0^2 - 2K_q \varphi_{\text{SAT}}} \quad (14)$$

and

$$W_{\text{SAT}} = \frac{1}{\sqrt{M_0^2 - 2K_q \varphi_{\text{SAT}}}} \quad (15)$$

For a memristor;

$$M_0 \geq M(q) \geq M_{\text{SAT}} \quad (16)$$

and

$$\frac{1}{M_{\text{SAT}}} \geq \frac{1}{M(q)} \geq \frac{1}{M_0} \quad (17)$$

$$W_{\text{SAT}} \geq W(\varphi) \geq W_0 \quad (18)$$

3. The new memristor-based active low-pass filter and its dynamic model

The memristor-based low-pass (LP) filter, which has been previously examined in literature [12, 13, 16, 20, 21] is given in Fig. 1.

The filter shown in Fig. 1 has an adjustable gain and adjustable cut-off frequency due to the fact that memristor memristance can change as a function of memristor charge. The filter gain and the filter cut-off frequency are, respectively,

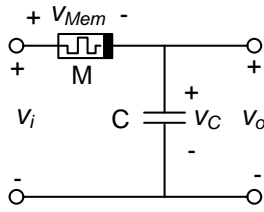


Fig. 1. The memristor-based low-pass filter.

The filter shown in Fig. 1 has an adjustable gain and adjustable cut-off frequency due to the fact that memristor memristance can change as a function of memristor charge. To adjust memristor charge, a tuning circuit can be used [19].

The filter gain and the filter cut-off frequency are, respectively,

$$G_{LPdB} = 20 \log_{10} \left(\frac{(V_C)_{RMS}}{(V_{IN})_{RMS}} \right) = 20 \log_{10} \left(\frac{1}{\sqrt{1 + (\omega C \bar{M})^2}} \right) \quad (19)$$

and

$$f_c = \frac{\omega_c}{2\pi} = \frac{1}{2\pi \bar{M} C} \quad (20)$$

As seen from (19) and (20), both the cut-off frequency and the filter gain vary as a function of memristor memristance. In this paper, we aimed to obtain a memristor-based low-pass filter with adjustable gain but with a constant cut-off frequency. The proposed LP filter is shown in Fig. 2. That parallel R-C circuit in the feedback path provides a constant cut-off frequency to the filter and also parallel resistor helps to get rid of the DC offset at the output and prevents the op-Amp from saturation at low frequencies. The new topology in Fig. 2 is to be analyzed in this section.

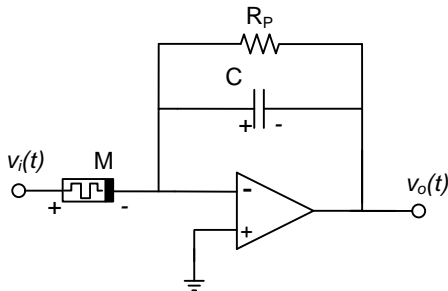


Fig. 2. Active low-pass filter with parallel resistance R_p

The dynamic model of the new filter is as the follows. The capacitor voltage of the filter:

$$\frac{dv_C}{dt} = -\frac{v_C}{R_p C} + \frac{v_{in}}{M(q)C} \quad (21)$$

If the memristor is not saturated;

$$i_{Mem} = \frac{dq_{Mem}}{dt} = \frac{v_{in}}{M(q)} \quad (22)$$

If the memristor is saturated and $i_{Mem} > 0$;

$$i_{Mem} = \frac{dq_{Mem}}{dt} = \frac{v_{in}}{M_{sat}} \quad (23)$$

If the memristor is saturated and $i_{Mem} < 0$;

$$i_{Mem} = \frac{dq_{Mem}}{dt} = \frac{v_{in}}{M_0} \quad (24)$$

For a sinusoidal signal, $v_{in} = V_m \cos(\omega t)$ and an unsaturated memristor, (21) turns into

$$\begin{aligned} C \frac{dv_C}{dt} + \frac{v_C}{R_p} &= W(\varphi) \cdot v_{in} \\ &= \frac{V_m \cos(\omega t)}{\sqrt{M_0^2 - 2K_q \varphi(0) - \frac{2K_q V_m}{\omega} \sin(\omega t)}} \end{aligned} \quad (25)$$

4. Small-signal analysis of proposed active Filter

To the best of our knowledge, (25) does not have an exact solution for sinusoidal input since it is highly nonlinear. Even symbolic math programs have been unable to solve this differential equation. In this section small-signal analysis of the new topology shown in Fig. 2 is done.

For the sinusoidal input signal the input current of the new filter by considering (25) is defined as

$$i_m = W(\varphi) v_{in} = \frac{V_m \cos(\omega t)}{\bar{M} \sqrt{1 - \frac{2K_q V_m}{\bar{M}^2 \omega} \sin(\omega t)}} \quad (26)$$

where $\bar{M} = \sqrt{M_0^2 - 2K_q \varphi(0)}$ is average memristance of memristor and $\varphi(0)$ is the average memristor charge for an electrical period.

To find solution of (21), a Maclaurin series expansion of (26) is found. The following Maclaurin series is used for this purpose:

$$\frac{1}{\sqrt{1-x}} = \sum_{n=0}^{\infty} (x)^n (-1)^n \binom{-1/2}{n} \quad (27)$$

For small x ($x \ll 1$):

$$\frac{1}{\sqrt{1-x}} \cong 1 + \frac{x}{2} \quad (28)$$

The input current given in (26) can be approximated using a Maclaurin series:

$$\begin{aligned} i(t) &\cong \frac{V_m \cos \omega t}{\bar{M}} \left(1 + \frac{K_q V_m}{\omega \bar{M}^2} \sin(\omega t) \right) \\ &\cong \frac{V_m}{\bar{M}} \cos(\omega t) + \frac{K_q V_m^2}{2\omega \bar{M}^3} \sin(2\omega t) \end{aligned} \quad (29)$$

Then, (25) turns into

$$\begin{aligned} C \frac{dv_c}{dt} + \frac{v_c}{R_p} &= W(\varphi) \cdot v_{in} \\ &= \frac{V_m}{\bar{M}} \cos(\omega t) + \frac{K_q V_m^2}{2\omega \bar{M}^3} \sin(2\omega t) \end{aligned} \quad (30)$$

and (30) is solvable. Its steady-state solution can be found using superposition in frequency domain and then switching back to time-domain.

The following trigonometric identities are also used to solve (30):

$$\cos(2\omega t) = 1 - 2\sin^2(\omega t) \Rightarrow \sin^2(\omega t) = \frac{1 - \cos(2\omega t)}{2} \quad (31)$$

$$\sin(2\omega t) = \cos\left(\frac{\pi}{2} - 2\omega t\right) = \cos\left(2\omega t - \frac{\pi}{2}\right) \quad (32)$$

In frequency domain, the feedback impedance and the capacitor voltage at angular speed ω are given as

$$\frac{1}{\bar{Z}_p} = \frac{1}{R_p} + \frac{1}{j\omega C} \quad (33)$$

$$\begin{aligned} \bar{Z}_p &= \frac{R_p}{j\omega C \left(R_p + \frac{1}{j\omega C} \right)} = \frac{R_p}{1 + j\omega R_p C} \\ &= \frac{R_p}{\sqrt{1 + (\omega R_p C)^2}} \angle -\arctan(\omega R_p C) \end{aligned} \quad (34)$$

The fundamental of the capacitor voltage is

$$\bar{V}_{c1} = \bar{Z}_p \bar{I}_1 \quad (35)$$

The fundamental of the capacitor voltage using (34) and (35) in time domain is given as

$$v_{c1}(t) = \frac{V_m R_p}{\bar{M} \sqrt{1 + (\omega R_p C)^2}} \cos(\omega t - \arctan(\omega R_p C)) \quad (36)$$

For the second harmonic, the angular frequency is 2ω and, the impedance of the second harmonic is

$$\begin{aligned} \bar{Z}_{p2} &= \frac{R_p}{j2\omega C \left(R_p + \frac{1}{j2\omega C} \right)} = \frac{R_p}{1 + j2\omega R_p C} \\ &= \frac{R_p}{\sqrt{1 + (2\omega R_p C)^2}} \angle -\arctan(2\omega R_p C) \end{aligned} \quad (37)$$

The second harmonic of the capacitor voltage is

$$\bar{V}_{c2} = \bar{Z}_{p2} \bar{I}_2 \quad (38)$$

The second harmonic of the capacitor voltage in time domain is given as

$$v_{c2}(t) = \frac{K_q V_m^2 R_p \sin(2\omega t - \arctan(2\omega R_p C))}{2\bar{M}^3 \omega \sqrt{1 + (2\omega R_p C)^2}} \quad (39)$$

Ignoring other harmonics than the second one and using superposition, the capacitor voltage becomes

$$\begin{aligned} v_c(t) = v_{c1}(t) + v_{c2}(t) &= \frac{V_m R \cos(\omega t - \arctan(\omega R_p C))}{\bar{M} \sqrt{1 + (\omega R_p C)^2}} \\ &+ \frac{K_q V_m^2 R_p \sin(2\omega t - \arctan(2\omega R_p C))}{2\bar{M}^3 \omega \sqrt{1 + (2\omega R_p C)^2}} \end{aligned} \quad (40)$$

The output voltage is

$$\begin{aligned} v_o(t) = -v_c(t) &= -\frac{V_m R_p \cos(\omega t - \arctan(\omega R_p C))}{\bar{M} \sqrt{1 + (\omega R_p C)^2}} \\ &- \frac{K_q V_m^2 R_p \sin(2\omega t - \arctan(2\omega R_p C))}{2\bar{M}^3 \omega \sqrt{1 + (2\omega R_p C)^2}} \end{aligned} \quad (41)$$

The filter gain is calculated from the fundamental of the input and output signals and is equal to

$$|G| = \frac{(V_o)_{RMS}}{(V_I)_{RMS}} = \frac{R}{\bar{M} \sqrt{1 + (\omega R_p C)^2}} \quad (42)$$

The filter gain in dB

$$G_{dB} = 20 \log_{10} \left(\frac{R}{\bar{M} \sqrt{1 + (\omega R_p C)^2}} \right) \quad (43)$$

As seen from(43), the gain has a constant cut-off frequency and is equal to

$$f_c = \frac{\omega_c}{2\pi} = \frac{1}{2\pi R_p C} \quad (44)$$

The output voltage spectrum of proposed LP filter for small signals can be seen in Fig 3. using (41)

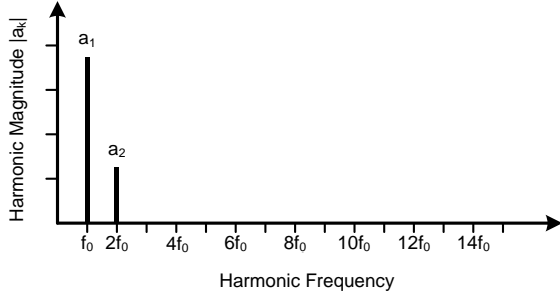


Fig. 3. Small signal frequency spectrum of the proposed low-pass filter output voltage.

For small signals, the total distortion of the low-pass filter can be assumed to be equal to

$$THD = \frac{(V_2)_{RMS}}{(V_1)_{RMS}} = \frac{K_q V_m}{2M^2 \omega} \sqrt{\frac{1 + (\omega R_p C)^2}{1 + (2\omega R_p C)^2}} \quad (45)$$

As it can be seen from (45), the total harmonic distortion increases while frequency decreases. The signal

amplitude should be small for a low distortion. This may be reached by keeping the ratio of the signal amplitude to the electrical angular frequency same. The distortion decreases at high frequencies since the memristor starts behaving as a linear time invariant circuit element.

5. Simulations of the proposed active low-pass filter

By considering analytical response and dynamical state equations of the proposed active LP filter, simulations are done and results are presented in same graphs for both methods to make comparing. Unless otherwise stated, during simulations parameters are taken as following: $C=50\text{nF}$, $R=10\text{k}\Omega$, $M_0=20\text{k}\Omega$, $M_{SAT}=500\Omega$, $q_{SAT}=2\mu\text{C}$, $\phi_{SAT}=20.5\text{mWb}$.

Time domain waveforms are given in Fig. 4 and Fig. 5. Memristor charge has some ripple and, therefore, the memristance has some ripple when low frequency signals are applied as seen in Fig. 4 (b). The memristor current is not sinusoidal at low frequencies and this can be seen in Fig. 4 (c) for 2 Hz. Corresponding I-V hysteresis loop for 2 Hz is shown in Fig. 4 (d).

If the filter frequency is 20 Hz, the memristor starts behaving almost as if a resistor, the ripple in the memristor charge and memristance are very low as shown in Fig. 5 (b). In this case, memristor current is almost sinusoidal as shown in Fig. 5 (c). Corresponding I-V loop is similar to LTI resistor's characteristic as seen in Fig. 5 (d).

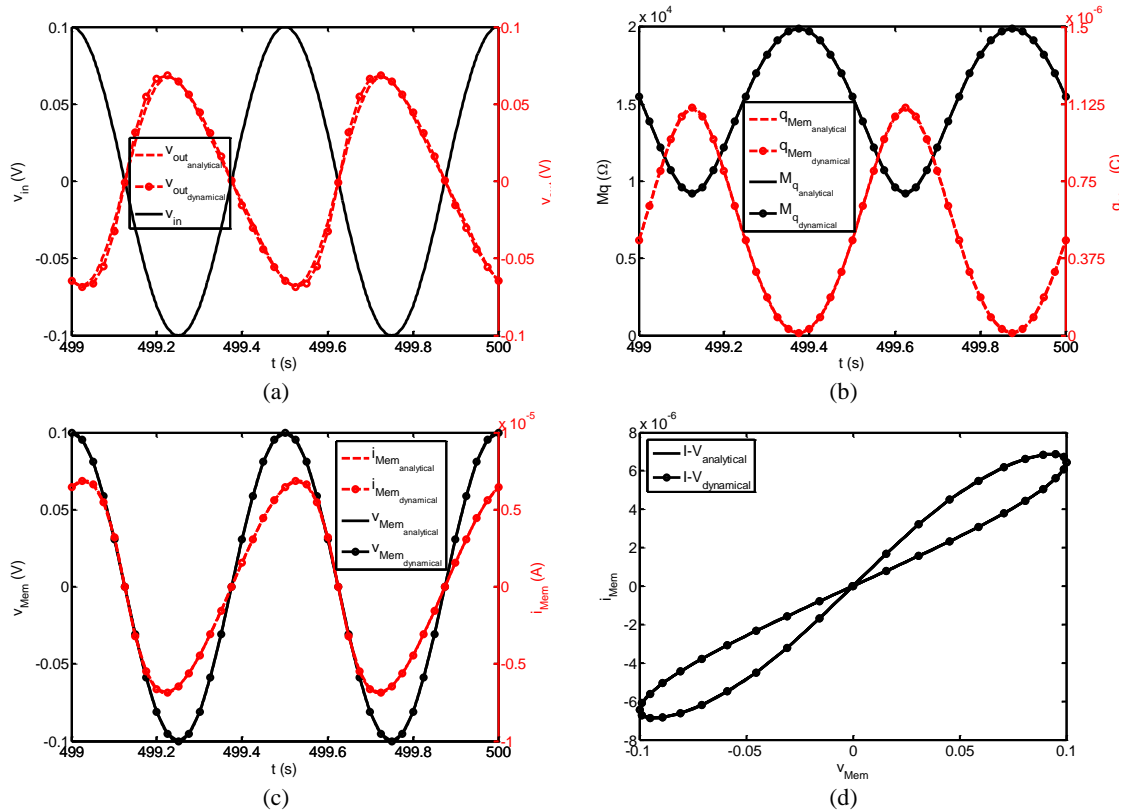


Fig. 4. Memristor-based active low-pass filter for $V_m=0.1\text{V}$, $\phi_0=0.4\phi_{SAT}$, $f=2\text{Hz}$ (a) filter input and output voltages (b) memristance and memristor charge (c) memristor voltage and current with function of time (d) memristor I-V characteristics.

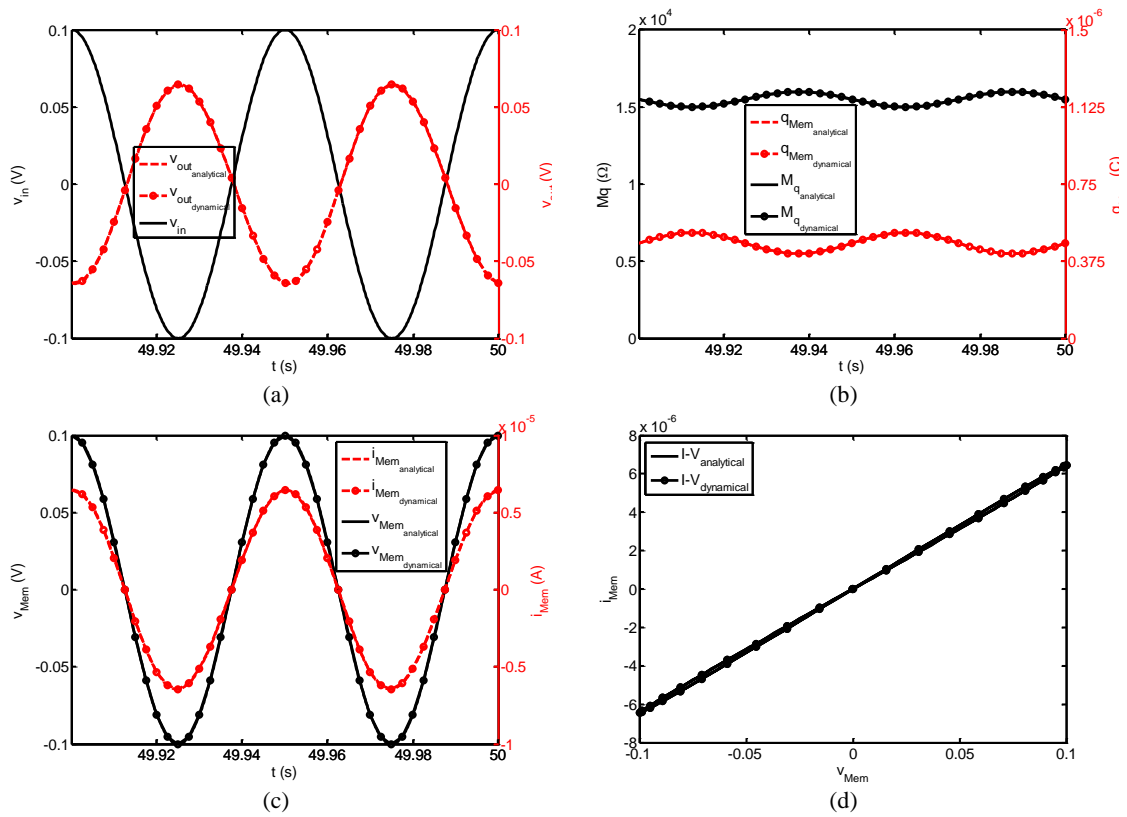


Fig. 5. Memristor-based active low-pass filter for $V_m=0.1V$, $\phi_0=0.4\phi_{SAT}$, $f=20Hz$ (a) filter input and output voltages (b) memristance and memristor charge (c) memristor voltage and current with function of time (d) memristor I-V characteristics.

The gain and the THD characteristics of the low-pass filter are given in Fig. 6 and Fig. 7. The filter has a constant cut-off frequency as seen in Fig. 6. At very-low frequencies, the small signal model results deviates from those of the dynamic model. The reason for this is that the filter memristor gets saturated and it is not sufficient to

represent the filter output voltage as the sum of the fundamental and the second harmonic, i.e. more harmonic terms are needed for a better accuracy. Also as seen in Fig. 7, at high values of memristor charge, there is also more distortion due to memristor saturation.

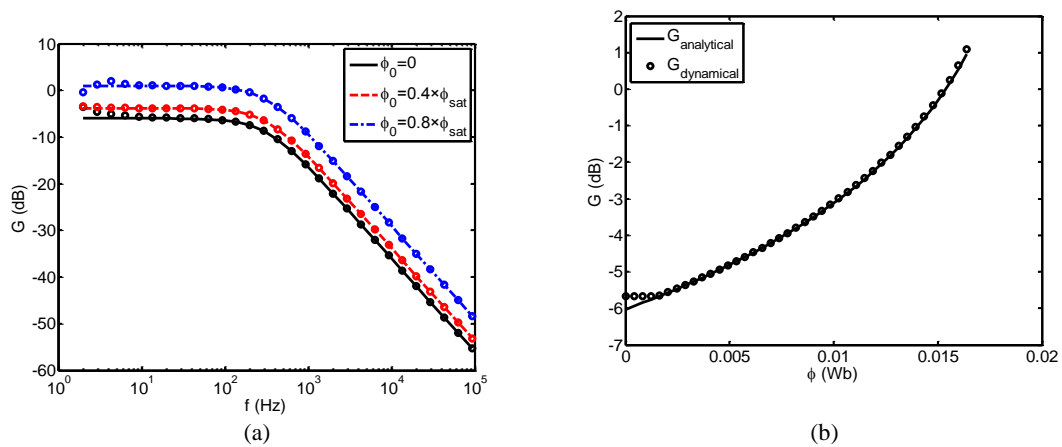


Fig. 6. Gain response of memristor-based active low-pass filter with parallel R_p for $V_m=0.1V$, a) respect to frequency (b) respect to ϕ_0 for $f=10Hz$

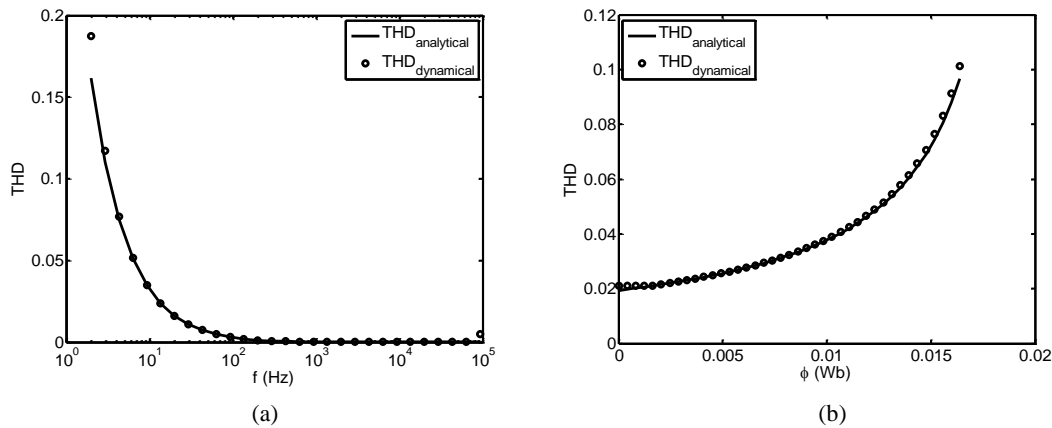


Fig. 7. Memristor-based active low-pass filter with parallel R_p THD characteristics for $V_m=0.1V$ a) respect to frequency $\phi_0=0.4\phi_{SAT}$ (b) respect to ϕ_0 for at $f=10Hz$.

6. Conclusions

In this paper, a TiO_2 memristor based active low-pass filter with an adjustable gain and a constant cut-off frequency is designed and analyzed. Dynamic model of the new LP topology is given. Due to the fact that the proposed memristor-based LP filter is highly nonlinear, it cannot be solved analytically. To find an approximate solution of the proposed filter, a small-signal analysis is done using Maclaurin series expansion for the first time in the literature. It should be also highlighted that it may be possible to solve memristor-based filters with more complex memristor or memristive system models using Taylor or Maclaurin series expansion methods. The accuracy of series expansion can be increased to the desired accuracy by using more terms if necessary. The filter is simulated using both the dynamic and small signal models. Results which are obtained by the two models are compared. It is proven that results obtained by the small-signal model are in good agreement with the numerical simulations.

Filter waveforms by respect to time are obtained and explained. Also, the frequency domain gain characteristics of the filter are obtained. As shown with simulations, the resistor-capacitor parallel feedback circuit provides a constant cut-off frequency and the memristor provides adjustable gain characteristic. Also the total harmonic distortion of the new memristor based low-pass filter is given as a figure of merit. THD and gain of the filter obtained by both dynamic and small-signal models are compared for small signals. Simulations showed that at low frequencies distortion is an important issue and performance decreases i.e. there is a drop in filter gain and THD decreases. Amplitude and angular frequency of the input voltage is found to be of importance. That's why the designer should know or predict the amplitude and frequency of the operating region. It has been also found that at low frequencies, the input signal magnitude should be limited for a low distortion.

References

- [1] L. Chua, Circuit Theory, IEEE Transactions on, **18**, 507 (1971).
- [2] D. B. Strukov, G. S. Snider, D. R. Stewart, R. S. Williams, Nature, **453**, 80 (2008).
- [3] L. O. Chua, S. M. Kang, Proceedings of the IEEE, **64**, 209 (1976).
- [4] R. Mutlu, "Solution of TiO_2 memristor-capacitor series circuit excited by a constant voltage source and its application to calculate operation frequency of a programmable TiO_2 memristor-capacitor relaxation oscillator."
- [5] Y. V. Pershin, M. Di Ventra, Circuits and Systems I: Regular Papers, IEEE Transactions on, **57**, 1857 (2010).
- [6] S. Shin, K. Kim, S.-M. Kang, Nanotechnology, IEEE Transactions on, **10**, 266 (2011).
- [7] O. Kavehei, A. Iqbal, Y. Kim, K. Eshraghian, S. Al-Sarawi, and D. Abbott, Proceedings of the Royal Society A: Mathematical, Physical and Engineering Science, **466**, 2175 (2010).
- [8] M. Qureshi, W. Yi, G. Medeiros-Ribeiro, R. Williams, Electronics letters, **48**, 757 (2012).
- [9] M. S. Qureshi, M. Pickett, F. Miao, J. P. Strachan, in Circuits and systems (ISCAS), 2011 IEEE international symposium on, 2011, pp. 2954-2957.
- [10] Y. V. Pershin, J. Martinez-Rincon, and M. Di Ventra, Journal of Computational and Theoretical Nanoscience, **8**, 441 (2011).
- [11] T. Driscoll, J. Quinn, S. Klein, H.-T. Kim, B. Kim, Y. V. Pershin, et al., Applied Physics Letters, **97**, 093502-093502-3, (2010).
- [12] T.-W. Lee, J. H. Nickel, (2012).
- [13] M. Mahvash, A. C. Parker, in Circuits and Systems (MWSCAS), 2010 53rd IEEE International Midwest Symposium on, 2010, pp. 989-992.
- [14] A. Ascoli, R. Tetzlaff, F. Corinto, M. Mirchev, M. Gilli, in Test Workshop (LATW), 2013 14th Latin American, 2013, pp. 1-6.

- [15] R. Raut, M. N. Swamy, *Modern Analog Filter Analysis and Design: A Practical Approach*: John Wiley & Sons, (2010).
- [16] Z. Chew, L. Li, *Electronics Letters*, **48**, 1610 (2012).
- [17] W. Wang, Q. Yu, C. Xu, Y. Cui, in *Communications, Circuits and Systems, 2009. ICCAS 2009. International Conference on*, 2009, pp. 969-973.
- [18] T. A. Wey, W. D. Jemison, *Circuits, Devices & Systems, IET*, **5**, 59 (2011).
- [19] Ş. Ç. Yener, R. Mutlu, H. H. Kuntman, *Informacije MIDEM - Journal of Microelectronics, Electronic Components and Materials*, **44**(2), 109 (2014).
- [20] S. C. Yener, R. Mutlu, H. Kuntman, in *Radioelektronika*, 15-16 April 2014, pp. 1-4.
- [21] S. Ç. Yener, R. Mutlu, H. Kuntman, in *22nd Signal Processing and Communications Applications Conference (SIU 2014)*, 23-25 April 2014, pp. 2027-2030.
- [22] W. Wang, Q. Yu, C. Xu, Y. Cui, in *2009 International Conference on Communications, Circuits and Systems, 2009*, pp. 969-973.

*Corresponding author: syener@sakarya.edu.tr